Incorporation of fast laser beam shunting and a broadband polarizer in the MAST Thomson scattering systems

M. J. Walsh, P. G. Carolan, A. C. Darke, M. R. Dunstan, M. J. Forrest, et al.

Citation: Rev. Sci. Instrum. **75**, 3909 (2004); doi: 10.1063/1.1781377
View online: http://dx.doi.org/10.1063/1.1781377
View Table of Contents: http://rsi.aip.org/resource/1/RSINAK/v75/i10
Published by the American Institute of Physics.

Incorporation of fast laser beam shunting and a broadband polarizer in the MAST Thomson scattering systems

M. J. Walsh,[a] P. G. Carolan, A. C. Darke, M. R. Dunstan, M. J. Forrest, R. B. Huxford,[b] R. O'Gorman,[c] K. Pechstedt, S. L. Prunty,[c] and R. Scannell[c]
EURATOM/UKAEA Fusion Association, Culham Science Centre, Abingdon, Oxfordshire OX14 3DB, United Kingdom

(Presented on 20 April 2004; published 12 October 2004)

Both ruby laser (300 points) and NdYAG laser (19 points) Thomson scattering systems are used on MAST. Fast nonlinear optical switching shunts laser beams from the four 50 Hz NdYAG lasers to obtain coaxial plasma illumination. The technique allows for future expandability to many laser systems. The ruby laser system is used in parallel. A broadband thin-plate polariser, based on nanotechnology, has been incorporated in the collection optics. It has a wide field of view and it almost halves the detected laser stray light and plasma background for both laser spectral regions. This allows much of the collection optics to function effectively in both spectral regions simultaneously. [DOI: 10.1063/1.1781377]

I. OPTICAL SHUNTING

The MAST[1] TS system[2,3] has been designed to handle up to eight, 50 Hz, 1.2 J, Nd:YAG lasers. At present, four of these lasers are implemented and these can be operated in several temporal modes such as burst, overlap or equispaced, see Fig. 1. Spatial sampling is across a maximum of 54 points, although the present arrangement has only 19 spatial points populated.

Using up to eight lasers to illuminate a line through a large tokamak such as MAST gives rise to overlap issues. In essence, the physical geometry of many lasers does not easily lend itself to a minimal area footprint. These beams can be arranged to lie behind each other, as seen by the collection optics. This works well in the focal plane of the lasers but outside this region the lasers gradually take up more and more physical space and hence can sample different parts of the plasma volume.

To minimize the multiple-laser footprint across the extended scattering length (1.5 m) requires a special arrangement of the lasers. A beam combining technique was created to send pairs of the lasers co-axially into the plasma. This scheme employs high performance polarizing optics to combine each pair of orthogonally polarized laser beams, and a fast switching electro-optic KD*P crystal device to switch the polarization orientation of alternate pulses.

An outline is shown in Fig. 2. It is seen that both lasers enter with vertical polarization. Laser 2 is prepared for the thin-film polarizer (TFP) by rotating the beam using a polarization rotator. This then passes through the TFP and is subsequently returned to the original vertical polarization with an appropriately timed pulse (~6.5 kV) on the Pockel's cell (PC). Laser 1 on the other hand is directly reflected off of the TFP and passes through the PC and hence lasers 1 and 2 are now made co-axial.

The high-voltage driver is designed to run at approximately 100 Hz into the capacitive load of the PC. To avoid degradation of the cell over time; a high voltage is applied to both terminals normally and then the high-voltage is switched to ground when a polarization rotation event is imminent. The rise-time to switch the cell to ground is of the order of nanoseconds. However, the recharge time using the present driver (few watts power) is about 5 ms. This information is important when using the lasers in burst-mode as the order of firing is critical. By firing laser 1 first, laser 2 can follow at any time down to ns after. As long as laser 1 repeats at a time greater than about 5 ms, the PC will be ready for the next pulse and so the whole process can be repeated. The repeat time of the present lasers is 20 ms. The implemented system is limited by the data collection ADC retrigger time of about 1.5 micro-seconds and burst mode is regularly used with timing spacing of 50–200 micro-seconds for the study of edge localized modes (ELMs) and other rapid target plasma events. This switching of the PC is accurately synchronized and triggered using the same pulse that fires the relevant laser, allowing multiple lasers to be bunched very closely together without significant timing or triggering errors.

Special consideration has to be taken in this design in dealing with the problems of high power loading, back reflections and optical damage threshold with each laser outputting approximately 160 MW/cm^2. Use of TFPs avoids the back reflection problem from the beam combiner, and other components are tilted slightly. All of these components are able to handle the power densities required. Issues such as stress-induced effects and thermal loading on the components have also to be considered. The PC chosen has a very low absorption factor of 0.003/cm and neglecting cooling, the temperature increase for each laser pulse applied is only

[a]Walsh Scientific Culham Science Centre, Abingdon, Oxfordshire OX14 3EB, UK; electronic mail: michael.walsh@ukaea.org.uk
[b]RBH Optics, Burgess Hill, West Sussex RH15 8 HL, UK.
[c]Department of Electrical & Electronic Engineering, University College Cork, Association EURATOM-DCU, Ireland.

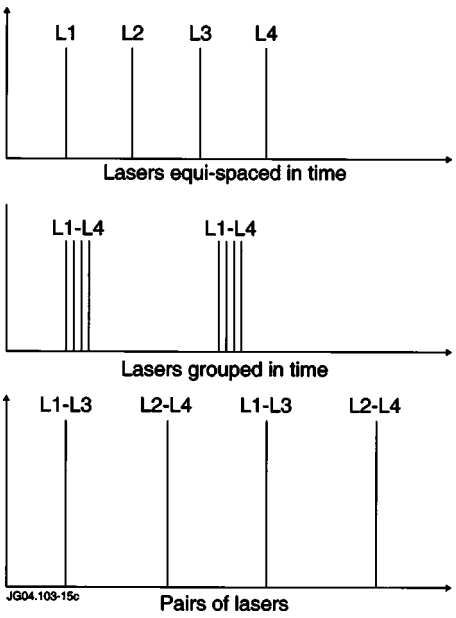

FIG. 1. Different modes of operation possible with the lasers setup as on the MAST Tokamak.

about 6 milli-degrees C (assuming a 3 mm top-hat beam radius). The present system is required to run for ~5 s on the MAST tokamak and in this period the temperature rise inside the PC is estimated to reach approximately 3 degrees while the redistribution of the heat within the cell will be small (redistribution time ~15 s). Crystals of this type typically have very low fracture toughness,[4] in this case, $\sim 0.09 \times 10^6$ $Nm^{3/2}$. Using a simple approximation for the allowable stress levels, it is found that a maximum temperature difference across the crystal of about 6 degrees may be enough to cause failure (assuming 100 μm surface defection scale-length). This means that expansion to accommodate more lasers, or even running the system for long periods of time would need more detailed analysis. The system installed on MAST has been in operation for thousands of plasma pulses and works routinely with no problems.

This resultant system is sufficiently compact that it can be viewed as a single 100 Hz-laser source but with the flexibility of varying the timing between pairs of pulses. Future enhancements could include combining four or more lasers.

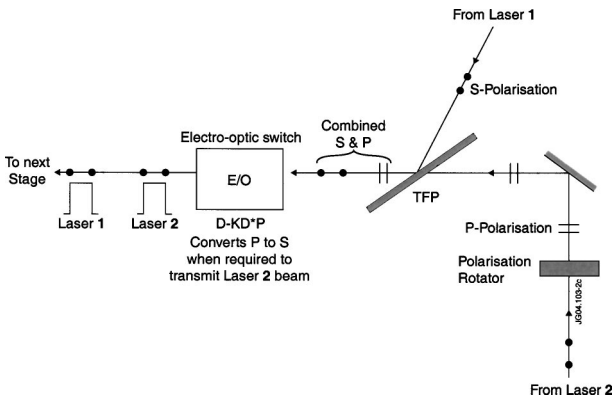

FIG. 2. Beam combining scheme showing the arrangement of the lasers and the main components used to couple the laser light to the next stage which in this case is via mirrors to the plasma target.

II. BROADBAND POLARIZERS IN COLLECTION OPTICS

Use of a good quality polarizer in the collection lens of the MAST Thomson scattering[3] system provides several advantages. First, it reduces background plasma light by a factor of ~2 and hence increases the signal to noise of the measured signals; second, it reduces stray light, advantageous when using Rayleigh scattering for density calibration and rejects unwanted orthogonal components in Raman calibrated systems, making for more straightforward calibration. It also assists in accurate calibration of the wavelength channels by limiting the light through the system to the polarization that is produced from Thomson scattering.

As described previously,[3] the MAST Thomson scattering system is made up of two systems; one high-resolution system based on a ruby laser and image intensifier/CCD type detection and another lower resolution system based on a Nd:YAG laser and using avalanche-photodiode technology. This means that the range of wavelength used by the combined systems extends from 550 to 1080 nm. Due to the geometry and the large size of the MAST load-assembly, the light is collected across an angular range of $\pm$21 degrees and the minimum size of the aperture is just under 180 mm in diameter. The light from any individual spatial point in only ~2.4 degrees, f/12.

For the polarizer to be of use it should have a transmission well above 80% for the preferred polarized light; rejection of unwanted polarization, or contrast, should be better than 5:1 minimum for background light suppression and better than 100:1 for Raman scattering calibration. Options for polarizers are numerous going from Brewster plates, calcite/crystal prisms, sheet to the traditional wire-grid approach. Given the size of the aperture and the space available the options that are available at a sensible cost are limited regardless of whether this is a retrofit or an original design.

While Brewster plates are excellent on wavelength response, they are large and bulky; they can suffer from image walk-off and several plates are required to get a good rejection. Calcite prisms on the other hand have excellent performance in all areas but implementation of these at any relevant part of the system would be prohibitive in terms of cost and size. Sheet polarizers are thin, cheap, high transmission, good rejection, minimum optical impact, but they only work in a narrow wavelength range which is not acceptable for even a single wavelength laser TS system. Finally, there is the option of the wire-grid polarizer. Wire-grids have been used extensively as polarizers in the infrared. Advances in nanotechnology now allow their application in the visible spectrum. Here, we explore the use of substrate based wire-grid polarizers. The wire-grid, see Fig. 3, sample was obtained from Moxtek Inc. The grid is made of high purity Aluminium wires supported by a Corning 1737F-glass substrate. The grid-spacing, $g \sim 144$ nm, the wire thickness, $2a \sim 65$ nm and substrate thickness $t \sim 0.7$ mm.

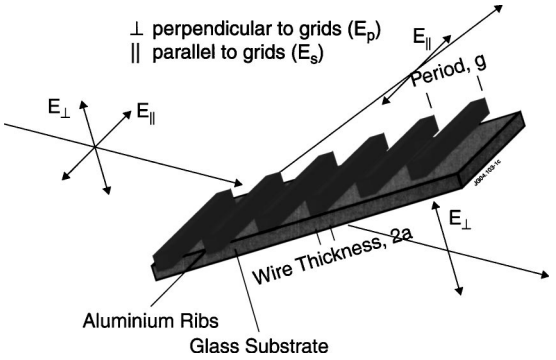

FIG. 3. Schematic of the wire-grid polarizer. In the polarizer used, $2a \sim 65$ nm and $g \sim 144$ nm.

III. RESULTS

The transmission was measured for a wavelength-range of 500–1090 nm for angles of incidence, $\theta = 0°$, 10°, 20°, and 25° degrees. The transmission of the capacitive grid (polarization perpendicular to grids), $T_\perp$, as shown in Fig. 4, is about 90%, while the transmission of the inductive grid (polarization parallel to grids), $T_\parallel$, is less than 0.2% over the whole wavelength range. As the angle of incidence increases, the capacitive and inductive transmittances both decrease. Also, $T_\perp$ varies between 85% and 94% within the wavelength range considered, while $T_\parallel$ lies in a range of 0.06%–0.17% (see Fig. 5). The change in $T_\parallel$ with incidence angle is negligible in absolute terms. In addition, it is found that the contrast increases slightly with the angle of incidence.

In summary, this wire-grid polarizer provides excellent transmission, $T_\perp$, for the E-field perpendicular to the strips,

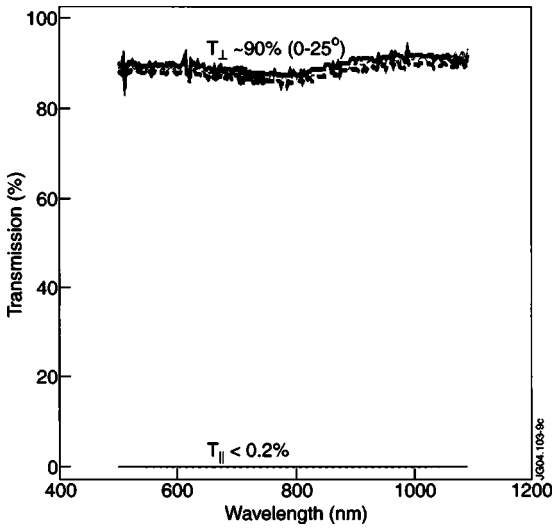

FIG. 4. Capacative (perpendicular to grids) and inductive (parallel to grids) transmissions of the wire-grid polarizer for a range of different angles, varying from 0° to 25°. The variation with angle is small with the 0° case being the highest.

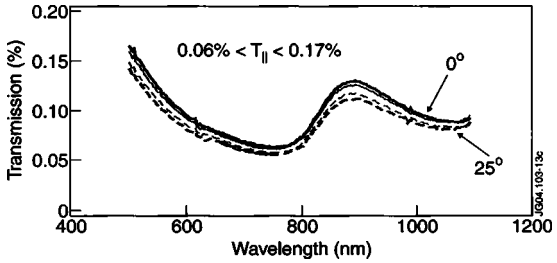

FIG. 5. Detailed view of the inductive transmission of the grids for a varying from 0° to 25°.

of around 90%, and a value of $T_\parallel$ of less than 0.2%. Also, the corresponding contrast is at least a factor of five higher than what is required.

The Moxtek wire-grid polarizer comes in a maximum size of 90 mm × 90 mm. The collection lens has a diameter of 180 mm. Therefore, a mosaic of four wire-grids can be fixed in front of the collection lens. The interspace loss is ~2%. As the transmission does not depend on whether the wave is incident in the wire or in the substrate side, the wire-grids are chosen to face the collection lens system, hence reducing the risk of damaging the delicate wires.

Two approaches can be taken to find the theoretical transmittance through a wire-grid supported by a substrate; diffraction grating theory[5] and transmission-line theory.[6] It is well known that the equations describing electromagnetic wave propagation in a homogeneous medium as described by Maxwell's equations are mathematically identical to those describing wave propagation on a transmission line. In principle, therefore, transmission-line theory can be used to find the transmittances of a wire-grid. Using the standard models for capacitive and inductive grids,[7,8] it is found that the transmission of the capacitive grid (main transmission) agrees well while the transmission-line model of the inductive grid significantly underestimates the measured performance indicating that the standard accepted model available in the literature needs updating.

It is beyond the scope of this article to go into these modifications other than to point out that the predicted transmissions for the polarization parallel to the wires is too high by approximately two orders of magnitude.

ACKNOWLEDGEMENTS

This work was jointly funded by UK Engineering and Physical Sciences Research Council and Euratom. We are indebted to the MAST team and, in particular, A. W. Morris and B. Lloyd.

[1] B. Lloyd *et al.*, Nucl. Fusion **43**, 1665 (2003).
[2] M. J. Walsh *et al.*, Rev. Sci. Instrum. **70**, 742 (1999).
[3] M. J. Walsh *et al.*, Rev. Sci. Instrum. **74**, Part 11, 1663 (2003).
[4] D. Eimerl, IEEE J. Quantum Electron. **QE-23**, 2238 (1987).
[5] X. J. Yu and H. S. Kwok, J. Appl. Phys. **93**, 4407 (2003).
[6] R. W. Stobie and M. J. Dignam, Appl. Opt. 12 (1973).
[7] L. B. Whitbourn and R. C. Compton, Appl. Opt. **24**, 217 (1985).
[8] D. Veron and L. B. Whitebourn, Appl. Opt. **25**, 619 (1986).